Dendrochronologia 76 (2022) 126016

Contents lists available at ScienceDirect

Dendrochronologia

journal homepage: www.elsevier.com/locate/dendro

Investigating the potential for Southern Hemisphere climate reconstruction using stable isotopes in Tasmanian tree rings

Zachary Grzywacz [a,*], Amy Hessl [a], Kevin Anchukaitis [b], Shikha Sharma [a], Michael N. Evans [c], Scott Nichols [d]

[a] Department of Geology and Geography, West Virginia University, Morgantown, WV, USA
[b] School of Geography, Development and Environment and Laboratory of Tree-Ring Research, University of Arizona, Tucson, AZ, USA
[c] Department of Geology and Earth System Science Interdisciplinary Center, University of Maryland, College Park, MD 20742, USA
[d] School of Biological Sciences, University of Tasmania, Hobart, TAS, Australia

ARTICLE INFO

Keywords:
Tree-ring stable isotopes
Dendroclimatology
Southern hemisphere
Tasmania
Tree
Rings

ABSTRACT

Few annually dated stable isotope records exist across Oceania. Stable carbon and oxygen isotope ratios have the potential to enhance climate reconstructions currently reliant on tree ring width chronologies. The purpose of this study is to explore the sources of variability in a stable oxygen isotope chronology derived from *A. selaginoides* from Mount Read, Tasmania. This high elevation site receives abundant rainfall throughout the year and is ~130 km from the Global Network of Isotopes in Precipitation (GNIP) site at Cape Grim. We crossdated 10 new tree core samples against an existing ring width chronology (954–2011 CE) and analyzed the $\delta^{18}O$ from the individual rings for the period 1960–2018. Using high resolution (0.25 degrees) climate data and ECMWF ERA5 reanalysis data, we disentangled the effects of local climate and source region on the isotopic signatures recorded in the annual rings. In addition, we used HYSPLIT backward trajectory analysis to characterize the source region of precipitation to Mount Read and whether the source region has influence over the $\delta^{18}O_{TR}$ series. Median $\delta^{18}O_{TR}$ ($n = 10$) is correlated with local temperature and vapor pressure deficit in the early growing season. In addition, spatial correlations reveal that median $\delta^{18}O_{TR}$ is positively correlated with temperature and negatively correlated with precipitation in the source region. However, measurements of $\delta^{18}O_{TR}$ exhibit high inter-tree variation, particularly between 1960 and 1990. Our results indicate that this $\delta^{18}O_{TR}$ proxy may provide additional information about past moisture conditions during the growing season, potentially contributing to more robust reconstructions of the Southern Hemisphere climate dynamics; however, additional sampling may be necessary to resolve inter-tree variation in $\delta^{18}O_{TR}$.

1. Introduction

Tree ring data are a source of high-resolution climate information for the Southern Hemisphere and have improved our understanding of synoptic scale climate (Abram et al., 2014; Villalba et al., 2012; Zi-Yin et al., 2010). Stable isotopes from tree rings could provide additional climate information, particularly where ring width is weakly correlated with climate variables (McCarroll and Loader, 2004). Several multi-millennial tree ring records exist for the Southern Hemisphere (Allen et al., 2017a, 2017b; Boswijk et al., 2006; Cook et al., 1991; Lara and Villalba, 1993), yet there has been limited application of tree ring stable isotopes for climate reconstruction outside of South America (Lavergne et al., 2016; Pearman et al., 1976; Roig et al., 2006). Oxygen isotopes in tree rings ($\delta^{18}O_{TR}$) are a promising source of information about past climate, though the effects of precipitation source region, local moisture, and tree physiology on $\delta^{18}O_{TR}$ can be complex (McCarroll and Loader, 2004; Porter et al., 2014; Treydte et al., 2014).

Generally, oxygen isotopes in tree rings follow distinct trends for temperature and precipitation. Higher temperatures and evaporation typically result in more enriched $\delta^{18}O_{TR}$ values through the influence of $\delta^{18}O$ of precipitation and evaporative enrichment (Dansgaard, 1964). The $\delta^{18}O$ of precipitation ($\delta^{18}O_P$) is dependent upon the $\delta^{18}O$ of the source water and the distance moisture has traveled from the source region. While there is not a 1:1 relationship between $\delta^{18}O_P$ and distance from source water, $\delta^{18}O_P$ becomes more depleted the further from the source water as it undergoes Rayleigh distillation which depletes $\delta^{18}O_P$.

* Corresponding author.
E-mail address: zackgrzywacz@gmail.com (Z. Grzywacz).

https://doi.org/10.1016/j.dendro.2022.126016
Received 3 June 2022; Received in revised form 30 September 2022; Accepted 5 October 2022
Available online 15 October 2022

Consequently, precipitation generally has a negative relationship with $\delta^{18}O_{TR}$. However, these effects can also be influenced by source region, as a polar source region will provide more depleted moisture, and a tropical source region will be more enriched. Seasonal effects will also influence the recorded $\delta^{18}O$ value, as higher temperatures result in an enriched $\delta^{18}O$ value in the summer, and the source region of precipitation may change with the seasons. Empirically, local moisture conditions and the origin of air masses are often the strongest influences on the $\delta^{18}O_{TR}$ chronology (McCarroll and Loader, 2004; Meier et al., 2020; Treydte et al., 2014).

Assuming that there is a strong relationship between the $\delta^{18}O$ of precipitation ($\delta^{18}O_P$) and $\delta^{18}O_{TR}$, it is possible to reconstruct historical temperature variations using $\delta^{18}O_{TR}$, and this has been achieved in South American mid-latitude sites (Lavergne et al., 2016; Roig et al., 2006). However, in Tasmania, $\delta^{18}O_P$ does not have a strong relationship with surface temperature (Treble et al., 2005). $\delta^{18}O_{TR}$ records can be difficult to interpret, given the influence of multiple climate variables at multiple scales on the final $\delta^{18}O$ value recorded in tree rings. It is possible that, in cases where the $\delta^{18}O_{TR}$ chronology is noisy, climate dynamics that control regional conditions may be the strongest influencing factor on the signal (Meier et al., 2020). Expanding the use of this method to new tree species and different regions would improve our ability to interpret these series and bolster the ability of tree-ring proxies to contribute to Southern Hemisphere climate reconstructions.

In this study, we investigated the influence of Southern Hemisphere climate measures on the $\delta^{18}O_{TR}$ value of Southern Hemisphere trees. Given previous relationships between local climate and $\delta^{18}O_{TR}$, the ideal site for this type of study is in a mid-latitude region with abundant precipitation (Treydte et al., 2014). *Athrotaxis selaginoides*, a conifer endemic to Tasmania, is long-lived with some individuals persisting for 1000 years or more, and subfossil wood suggesting preservation of up to 2000 years (Allen et al., 2017a, 2017b). *A. selaginoides* develops consistent annual rings, but ring width measurements only weakly reflect local climate variability (Allen et al., 2017a, 2017b), indicating that stable isotope records have the potential to contribute new climate information not present in other tree-ring parameters. The purpose of this study is to explore the local to regional sources of variability in a stable oxygen isotope chronology derived from *A. selaginoides* from Mount Read, Tasmania.

2. Study area

A research team conducted tree ring sampling of live *A. selaginoides* trees near the summit of Mount Read (41.84° S, 145.54° E, 1123 m), located on the west coast of Tasmania, Australia during January 2020 (Fig. 1). The west coast of Tasmania is characterized by a moist climate, with cold winters and warm summers (Reid, 1998). Median annual rainfall on Mount Read is 3768.4 mm (Bureau of Meteorology, 2022), which is among the highest values in Tasmania. Rainfall peaks in winter, though monthly rainfall totals exceed 170 mm in all months. High levels of precipitation should strengthen the relationship between $\delta^{18}O$ of precipitation and $\delta^{18}O$ of soil water by limiting the fractionation effects of evaporation (Treydte et al., 2014). Mount Read has a peak elevation of 1123 m, placing it at the edge of *A. selaginoides*' elevation range. The forest at the site is located on a steep slope (20–45 degrees) and is classified as a cool temperate rainforest. Cool temperate rainforests, which mainly occur in Tasmania, are areas with high rainfall, mild summers, and cool winters, and mainly consist of evergreen tree species (Busby and Brown, 1994). The forest on Mount Read is composed mainly of *Athrotaxis selaginoides* and *Nothofagus cunninghamii*.

Fig. 1. Map of Tasmania that highlights the study site (Mount Read) as well as the source of GNIP measurements (Cape Grim).

3. Methods

3.1. Sample preparation and isotopic analyses

A research team collected 5 mm cores from 20 *A. selaginoides* trees on Mount Read. Three cores were collected from each tree to ensure that enough mass was present to perform isotope analysis. We recorded tree height, diameter at breast height (DBH), soil depth, canopy cover, and slope for each tree we sampled.

We mounted, sanded, dated, and measured all the cores gathered for each tree using standard dendrochronological methods (Stokes and Smiley, 1968). We measured and crossdated individual ring widths and tested the accuracy of these measurements and their dating by comparing them to measurement patterns in an existing crossdated chronology from Mount Read (Allen et al., 2017a, 2017b) using the software COFECHA (Holmes, 1983). The existing chronology covers the period 954 – 2011 CE and contains 50 ring width series (Appendix, Fig. S1A). For the purposes of comparing the stable isotope record developed here with a proxy derived from ring widths, we created a detrended ring width chronology, including the new series collected and measured in this study. We power transformed (Cook and Peters, 1997) and detrended the increment series using an age-dependent smoothing spline where the frequency response is set at 0.50 for a wavelength of 0.67 (2/3 length of each series). Residual values from the detrended series were combined in a mean-value chronology using Tukey's biweight robust mean. For subsequent analysis, we used the years 1960 – 2018 of the chronology, with a sample depth of 55 ring width series. For Southern Hemisphere tree ring samples, the "current" year includes the subsequent year's growing season months. Therefore, a sample assigned the year 1960 represents the growing season of September 1960 – February 1961. We did not treat the isotope data in any way related to the age of the samples, as there is little evidence pointing to a juvenile effect for $\delta^{18}O_{TR}$ (Leavitt, 2010), and the mean age or our samples in 1960 was 356.9 years.

For each tree with reliable dating (two cores correlate with the master chronology > 0.3), we used a rotary microtome to section individual rings into 20 μm shavings for the years 1960 – 2018. We stored shavings in polypropylene microcentrifuge tubes labeled with the year and tree ID. Rings that belong to the same tree were pooled by year to ensure enough mass was present to gather isotopic ratios. We used the Brendel et al. (2000) method to isolate the α-cellulose from the whole-wood samples, ideal for $\delta^{18}O_{TR}$ measurement. This method allows for batch sampling for efficiency and is designed for small-mass samples. Prior to isotope analysis, we placed 0.20 mg (+/- 0.02 mg) of each dried sample into a silver capsule. $\delta^{18}O$ in the cellulose samples was measured using high-temperature pyrolysis in a Costech HTG 02 elemental analyzer coupled with a Costech-IRMS (at the University of Maryland, College Park). The samples were measured against two standards, SAC (Sigma alpha cellulose) and AKC (Alaskan corn). We recorded all $\delta^{18}O_{TR}$ samples as the proportion of $^{18}O/^{16}O$ using per mil (‰) notation with respect to Vienna Standard Mean Ocean Water (VSMOW).

3.2. Analysis

To reduce the influence of outlying values, median values for each year were used to create a time series of $\delta^{18}O_{TR}$ and calculated bootstrapped 95% confidence intervals of the median values were calculated to provide a measure of variability. We calculated the expressed population signal (EPS), mean inter-tree correlation (Rbar), signal to noise ratio (SNR), and Gleichläufigkeit sign test (GLK) of the $\delta^{18}O_{TR}$ chronology to assess the strength of the common signal.

To assess the relationship between $\delta^{18}O_{TR}$ and measured $\delta^{18}O$ of precipitation, we performed Pearson correlations between $\delta^{18}O_{TR}$ and monthly measurements of $\delta^{18}O_P$ (September through February) from IAEA Global Network of Isotopes in Precipitation (GNIP) measurements of $\delta^{18}O_P$ at Cape Grim, Tasmania for 1979–2002 (IAEA/WMO, 2021). If $\delta^{18}O_P$ is strongly correlated with $\delta^{18}O_{TR}$, then variation in $\delta^{18}O_{TR}$ is likely influenced by source region conditions. However, if there is little to no significant relationship, then local moisture (measured as vapor pressure deficit or relative humidity) may be a stronger influence on $\delta^{18}O_{TR}$.

To assess local climate influences on $\delta^{18}O_{TR}$, we calculated correlations between our $\delta^{18}O_{TR}$ values and local climate conditions on Mount Read. We obtained rasterized climate data (precipitation, minimum and maximum temperature, relative humidity, vapor pressure deficit, solar radiation) from the Australian Bureau of Meteorology's SILO database (Jeffrey et al., 2001), recorded as daily values in netcdf format at 0.05×0.05-degree resolution (1960–2018). We created monthly averages (or totals for precipitation) based on daily SILO grids and extracted values for Mount Read via bilinear interpolation of the four closest cells to the study site (145.54, −41.84). We calculated correlations between the Mount Read $\delta^{18}O_{TR}$ and 3-month rolling averages of temperature, precipitation, vapor pressure deficit (VPD), relative humidity, and solar radiation at Mount Read for September through February. The seasonal correlations allowed us to determine if certain seasons influence the $\delta^{18}O_{TR}$ record more than others, thus those seasons could be well represented in any climate proxy produced by the tree-ring isotopes.

To understand the potential source region of precipitation for Mount Read, we calculated backward trajectories for Mount Read, Tasmania using the model HYSPLIT (Stein et al., 2015), accessible in the R environment through the package SplitR (Iannone, 2016). Using NCEP/NCAR reanalysis data (Kalnay et al., 1996; Department of Commerce, 1994) as atmospheric pressure inputs, we computed five-day backwards trajectories every six hours at 5-day intervals at 10 m elevation for September – February over the study period (1960–2018). We then summarized these trajectories by calculating the frequency of trajectories crossing 0.5-degree cells during the period of record. We log-transformed these trajectory frequencies to visualize Mount Read's source region of precipitation.

We used HYSPLIT backward trajectories (as above) to determine if there was any difference in moisture delivery between the years with the highest and lowest median $\delta^{18}O_{TR}$ to assess moisture delivery patterns associated with variation. We composited backward trajectories at Mount Read during the 15 years (top 25%) where the median $\delta^{18}O_{TR}$ was the highest as well as the 15 years (bottom 25%) where $\delta^{18}O_{TR}$ was the lowest. We then calculated anomalies from the mean conditions to determine how the source regions differ when $\delta^{18}O_{TR}$ was anomalous. This helped us determine if variation in $\delta^{18}O_{TR}$ can be partially explained by a difference in moisture delivery.

To observe which regional climate variables influence the $\delta^{18}O_{TR}$ series, as well as the specific areas where they are influential, we created spatial correlation maps between the $\delta^{18}O_{TR}$ series and regional climate variables. We downloaded the European Centre for Medium-Range Weather Forecasts (ECMWF) ERA5 reanalysis data (Bell et al., 2020; Hersbach et al., 2019) from the Copernicus Climate Change Service (C3S) Climate Data Store. We performed Pearson correlations between the $\delta^{18}O_{TR}$ series and spatial climate fields from ERA5 to assess any relationship with source region conditions. The ERA5 dataset spans 1950 to the present and is updated daily with hourly measurements. Monthly means have been pre-calculated by the ECMWF, which we used in our analyses. We used total precipitation and temperature at 2 m elevation for the years 1960 – 2018. For each variable, we extracted ERA5 spatial fields to an extent that includes the source region of precipitation to Mount Read as defined by the mean HYSPLIT analysis above. Then, for each cell, we correlated the climate fields with the $\delta^{18}O_{TR}$ series. We compared these spatial correlation maps to the HYSPLIT back trajectory summary to validate that the most influential areas are the source of precipitation over Mount Read. In addition, due to the monthly resolution of these data, we evaluated whether source region influence is stronger in certain seasons. For comparison, we calculated spatial correlations between ERA5 climate data with average Cape Grim

$\delta^{18}O_P$ for September – February for the years 1979 – 2002.

4. Results

4.1. Assessing Local Influences on $\delta^{18}O_{TR}$

We successfully sectioned 20 cores from 10 trees into individual years producing a total of 521 cellulose samples for isotope analysis. In the $\delta^{18}O_{TR}$ series, not every year is represented by all 10 trees, though every year is represented by at least 8 trees (mean sample size per year = 8.75 trees) thus exceeding the typical minimum sample depth of 4–6 cores per tree (Leavitt, 2010).

The $\delta^{18}O_{TR}$ values of the *A. selaginoides* trees have a low EPS (0.566) and rbar (0.130) for the period 1960 – 2018 (Table 1) relative to that of the ring width series EPS (0.965) and rbar (0.222). The series also has a low Gleichläufigkeit (GLK) value (0.555), otherwise known as the sign test, which is a measure of synchronicity between trees. The series shows weak, yet significant first-order and second-order autocorrelation (AC1 = 0.319; AC2 = 0.273). The mean of the *A. selaginoides* $\delta^{18}O_{TR}$ chronology for all years is 27.72‰ (sd = 0.87‰) with means for individual trees ranging from 26.83‰ to 28.28‰. Variability between trees is greater from 1960 to 1995 (sd = 0.97‰) than from 1996 to 2018 (sd = 0.71‰; Fig. 2A). Variability tightens from ~1980 – 1987, before widening again from ~1988 – 1995. No temporal trend was found in the data.

Median $\delta^{18}O_{TR}$ has weak but significant positive correlations in the early growing season with VPD (Fig. 3A; $r = 0.32$, $p < 0.05$ for Oct - Dec); temperature ($r = 0.27$, $p < 0.05$ for Oct - Dec); and solar radiation ($r = 0.30$, $p < 0.05$ for Oct - Dec). The correlation with Jan - Mar precipitation is also significant but weak ($r = 0.26$, $p < 0.05$). Standard deviation in the $\delta^{18}O_{TR}$ chronology is most strongly negatively correlated with VPD in Nov – Jan (Fig. 3B; $r = -0.27$, $p < 0.05$); temperature in Nov – Jan ($r = -0.29$, $p < 0.05$); solar radiation in Oct – Dec ($r = -0.41$, $p < 0.05$); and precipitation in Sep – Nov ($r = -0.27$, $p < 0.05$) and Jan – Mar ($r = -0.28$, $p < 0.05$). Both temperature ($r = -0.30$, $p < 0.05$) and solar radiation ($r = -0.26$, $p < 0.05$) exhibit negative correlations for the full Sep – Feb interval.

A. selaginoides ring width is positively correlated with irradiance in the Sep – Nov season (Fig. 3C; $r = 0.34$, $p < 0.05$). All other correlations between *A. selaginoides* ring width and local climate variables are not significant.

The only significant Pearson correlation between $\delta^{18}O_{TR}$ and Cape Grim $\delta^{18}O_P$ occurs in the 3-month period of Nov – Jan (Fig. 4, $r = 0.55$, $p < 0.05$) during the growing season. Correlations with Cape Grim $\delta^{18}O_P$ for all other seasons are not significant.

4.2. Assessing Influences of Source Region on $\delta^{18}OTR$

The difference in the HYSPLIT output between the top 25% of $\delta^{18}O_{TR}$ years and the bottom 25% of $\delta^{18}O_{TR}$ years is most prevalent in the region to the west of Tasmania (Fig. 5). High $\delta^{18}O_{TR}$ years show a consistent western mid-latitude influence, whereas low $\delta^{18}O_{TR}$ years have a stronger influence from the east and northeast of Tasmania.

Correlations between $\delta^{18}O_{TR}$ and regional climate variables reveal relationships in the source region of precipitation for Mount Read. Temperature is positively correlated with $\delta^{18}O_{TR}$ in some areas surrounding Tasmania (Fig. 6A). The most notable areas of significance for temperature are to the west of Tasmania, south of mainland Australia ($0.2 < r < 0.4$), immediately to the east of Tasmania ($0.2 < r < 0.4$), and over the mainland of Australia ($0.3 < r < 0.5$).

Precipitation is negatively correlated with $\delta^{18}O_{TR}$ immediately surrounding Tasmania to the west, as well as to the north in mainland Australia (Fig. 6C; $-0.5 < r < -0.2$). There are small areas where precipitation is positively, though weakly, correlated with $\delta^{18}O_{TR}$ in the Southern Ocean ($0.2 < r < 0.4$).

Correlations between Cape Grim $\delta^{18}O_P$ and regional climate variables reveal differences in source region influences from the $\delta^{18}O_{TR}$ series. The region displaying significant temperature correlations is remarkably different here, with the region to the northeast of Tasmania displaying strong (0.4 – 0.7) correlations between temperature and Cape Grim $\delta^{18}O_P$ (Fig. 6B). Precipitation shows a similar pattern of correlation with Cape Grim $\delta^{18}O_P$, with strong negative correlations (0.4 – 0.6) present to the west of Tasmania (Fig. 6D). It is important to note that, due to the lower number of observations (24 years vs. 59), the threshold to be considered a significant correlation ($p < 0.05$) requires a stronger relationship.

Table 1
Comparison between $\delta^{18}O_{TR}$ and the A. selaginoides ring width chronology, including the number of series, rbar (average interseries correlation), EPS (expressed population signal), SNR (signal to noise ratio), and GLK (Gleichläufigkeit sign test) for the period of instrumental record (1960 –2018).

Tree Ring Series	Series (n)	Rbar	EPS	SNR	GLK
$\delta^{18}O_{TR}$	10	0.130	0.566	1.302	0.555
A. selaginoides ring width	55	0.222	0.965	27.328	0.637

5. Discussion

5.1. Connectivity between $\delta^{18}O_{TR}$ and $\delta^{18}O_P$

Temperate forests with abundant, year-round moisture are theoretically optimal sites for climate reconstruction using oxygen isotope reconstruction (Treydte et al., 2014). Due to the limited fractionation of soil water and leaf water, one expects a strong relationship between $\delta^{18}O_P$ and $\delta^{18}O_{TR}$. With high rainfall every month, we expected *A. selaginoides* tree rings to yield a coherent isotopic signal suitable for regional climate reconstruction via stable oxygen isotopes. However, we found high variability in $\delta^{18}O_{TR}$ values between trees, low EPS (0.566), and low rbar (0.13), indicating weak interannual correlation between samples and a weak common signal (Table 1).

Paired $\delta^{13}C_{TR}$ measurements maintained relatively high EPS (0.791) and rbar (0.318) statistics (Grzywacz, 2021), indicating that crossdating and sample preparation were not a likely cause of the intertree variation. Other possible explanations for the variation between trees include disparate influence of the P é clet effect on individual trees under cool and wet conditions (Barbour et al., 2004), as well as factors such as rooting depth and complex topography altering $\delta^{18}O$ of soil water available to trees. Other explanations for variability include the influence of water storage from previous years, which is supported by significant first-order (0.319) and second-order (0.273) autocorrelation values observed here. Despite the high degree of inter-tree variability in $\delta^{18}O_{TR}$, there is a correlation with $\delta^{18}O_P$ at Cape Grim in the growing season ($r = 0.304$, $p = 0.01$), suggesting that some of the $\delta^{18}O_P$ signal is preserved in the tree rings.

5.2. Local conditions and $\delta^{18}O_{TR}$

The $\delta^{18}O_{TR}$ series is influenced by not only $\delta^{18}O_P$, but also by local climate conditions that influence rates of fractionation at the site. A common dominant control on $\delta^{18}O_{TR}$ is local moisture, usually measured by relative humidity (McCarroll and Loader, 2004). Because of the high level of year-round moisture availability at Mount Read, we expected local moisture effects to be minimal. Consistent with other studies (Grießinger et al., 2018; Lavergne et al., 2016; Porter et al., 2014), local temperature is significantly and positively correlated with $\delta^{18}O_{TR}$ in the early growing season (Oct – Dec $r = 0.27$, $p < 0.05$), though the strength of the relationship is weak. While some studies have used $\delta^{18}O_{TR}$ as a proxy for local temperature, the relationship here is not strong enough to support a temperature reconstruction. In a study of $\delta^{18}O_P$ and climate in Tasmania, Treble et al. (2005) also found a weak relationship between $\delta^{18}O_P$ and local temperature, so it is likely that

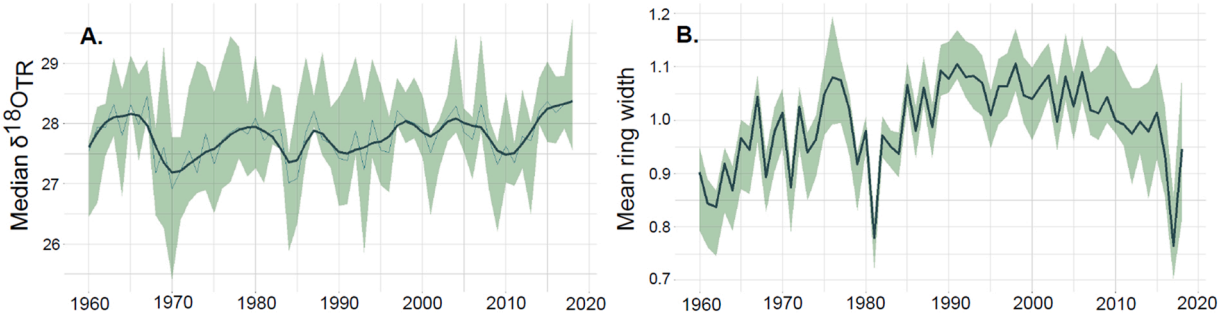

Fig. 2. Representations of A. selaginoides series of $\delta^{18}O_{TR}$ (A) and ring width (B) for 1960–2018. Dark green line is a spline calculated using a frequency response of 0.9 and a wavelength of 10 years of median $\delta^{18}O_{TR}$ in (A). In (B), dark green line is a 2/3 smoothing spline of mean ring width. Light green represents a 95% confidence interval in all plots. Light blue line in (A) is the measured median $\delta^{18}O_{TR}$.

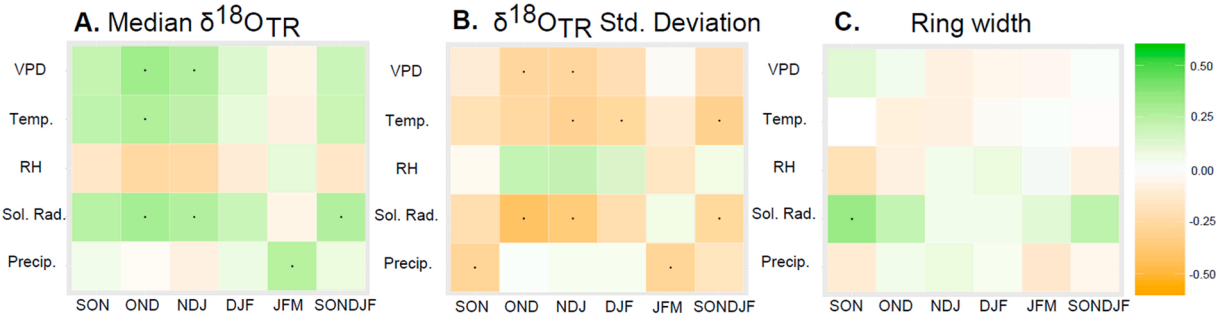

Fig. 3. Correlations between 3-month averages of climate variables at Mount Read and median $\delta^{18}O_{TR}$ (A), $\delta^{18}O_{TR}$ standard deviation (B), and ring width (C). Dotted squares indicate statistically significant correlations ($p < 0.05$).

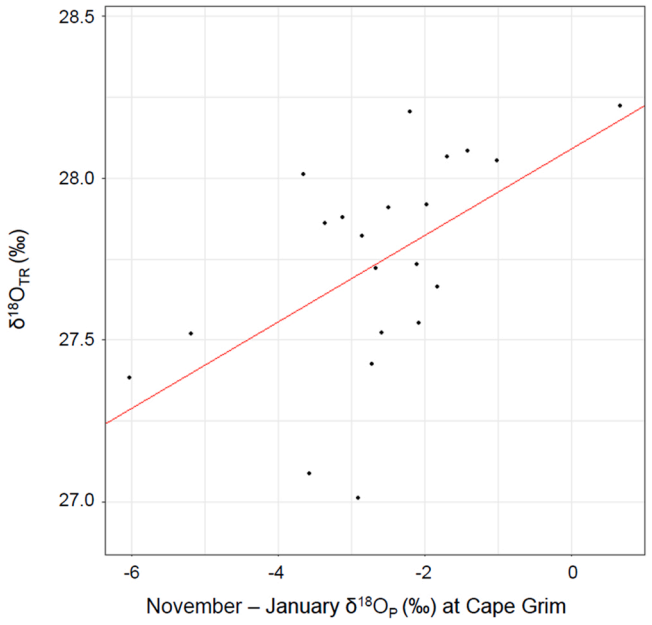

Fig. 4. δ18OTR plotted against November – January average of δ18OP at Cape Grim, Tasmania. Red line represents a regression between δ18OTR and November – January δ18OP (R-squared = 0.304, p = 0.01).

$\delta^{18}O_{TR}$ is influenced by multiple variables in this region.

Also as expected, $\delta^{18}O_{TR}$ is not significantly correlated with relative humidity over any 3-month period during September to February (Fig. 3). However, $\delta^{18}O_{TR}$ is weakly, but significantly correlated with VPD during Oct – Dec ($r = 0.32$, $p < 0.05$) and Nov – Jan ($r = 0.27$, $p < 0.05$), the drier portion of the year. This low correlation, when combined with the lack of a correlation with relative humidity, implies that local moisture is not a strong influence on $\delta^{18}O_{TR}$.

Surprisingly, we observed a positive relationship with precipitation amount ($r = 0.26$ for JFM). Treble et al. (2005) found that $\delta^{18}O_P$ is negatively related to precipitation in Tasmania; however, they also found numerous events where large amounts of rainfall are associated with average $\delta^{18}O_P$ values. Mean sea level pressure (MSLP) maps during heavy rainfall events show the potential for advection of air down the East coast of Australia to Tasmania (Treble et al., 2005). This phenomenon, observed mostly during the warm season, resulted in a low latitude moisture source more enriched than moisture from the mid- and high-latitudes. We conclude that the most likely explanation for the positive relationship we found between precipitation and $\delta^{18}O_{TR}$ is an overrepresentation of precipitation events originating from the lower latitudes during the January - March months.

Finally, $\delta^{18}O_{TR}$ is correlated with Cape Grim-derived $\delta^{18}O_P$, indicating a direct linkage between tree ring isotopes and actual measured $\delta^{18}O_P$ in source water. While not dominating the $\delta^{18}O_{TR}$ value, $\delta^{18}O_P$ is an influential source of variation in $\delta^{18}O_{TR}$, implying that the record is reflective of conditions that influence $\delta^{18}O_P$. When we also consider that local moisture conditions display some influence on the record during dry months, it is likely that the $\delta^{18}O_{TR}$ record is the result of a mix of signals from both the local scale and regional scale.

5.3. Source region dynamics

Climate conditions in the source region of precipitation are often reflected in $\delta^{18}O_{TR}$ (Porter et al., 2014; Treydte et al., 2014). $\delta^{18}O_{TR}$ shows a positive relationship with temperature in the Indian Ocean immediately to the south of mainland Australia (Fig. 6A; 35–45° S, 110–140° E). For precipitation, there is an area of strong negative correlation immediately to the west of Tasmania, slightly further east (Fig. 6C; 40–45° S, 135–145° E) than the region of correlation for temperature. The temperature~$\delta^{18}O_{TR}$ correlations show some influence

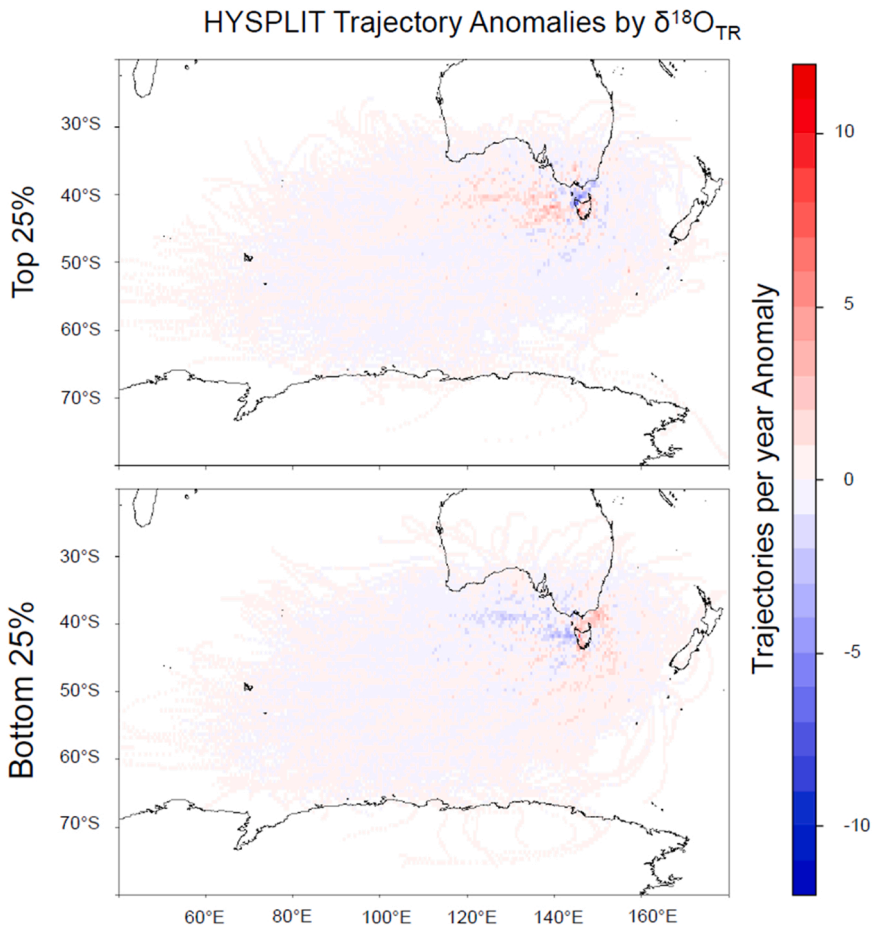

Fig. 5. Comparison of anomaly plots for HYSPLIT output between the top and bottom 25% of years by δ18OTR. Positive anomalies (red) represent areas that have a greater abundance of trajectories than the mean conditions, while negative anomalies (blue) represent areas with a lower abundance of trajectories than the mean conditions.

east of Tasmania in the Tasman Sea, while precipitation~$\delta^{18}O_{TR}$ correlations show minimal influence from the east. The direction of these correlations is consistent with known relationships between $\delta^{18}O_P$ and temperature and precipitation in the source region (McCarroll and Loader, 2004). Spatial correlations for the Cape Grim $\delta^{18}O_P$ data (Fig. 6) suggest that moisture to the northeast of Tasmania is influential in determining the $\delta^{18}O_P$ signal, while the area to the west is less influential.

We would expect $\delta^{18}O_P$ and $\delta^{18}O_{TR}$ to share similar relationships with regional climate. However, the climate~$\delta^{18}O_{TR}$ correlations and climate~$\delta^{18}O_P$ correlations are at best broadly similar in direction and regional influence (Fig. 6). Tasmania experiences occasional easterly winds (Hendon et al., 2007), which could explain the Cape Grim correlation pattern with temperature only to the east of Australia. It is possible that moisture that originates in the northeast, while more infrequent, is more enriched in $\delta^{18}O$ than most moisture delivered to Tasmania, and this strong $\delta^{18}O_P$ value influences the Cape Grim dataset. This result is consistent with the negative correlation with local precipitation (Fig. 3) and the observations of Treble et al. (2005). The $\delta^{18}O_{TR}$ and temperature relationship (Fig. 6A) shows a stronger influence over mainland Australia and less influence of temperatures to the east. Enriched precipitation from eastern sources occurring in heavy rain events (Treble et al., 2005) would mix with moisture storage already present at Mount Read, and much of it would run off before being incorporated into the trees, resulting in a more muted influence on the $\delta^{18}O_{TR}$ value. HYSPLIT trajectory anomalies by $\delta^{18}O_{TR}$ reveal that source moisture from the region to the west of Tasmania is associated with high $\delta^{18}O_{TR}$ (Fig. 5). Trajectories from other regions, specifically to the south and northeast of Tasmania are associated with low $\delta^{18}O_{TR}$. This could imply that years of low $\delta^{18}O_{TR}$ have a different source region from usual conditions, as west of Tasmania is the most common source region for Mount Read.

This difference in source region could be associated with a variety of factors, including dynamical processes such as the Southern Annular Mode (SAM), El Niño–Southern Oscillation (ENSO), and the Indian Ocean Dipole (IOD). The SAM exhibits positive and negative phases, marked by the north-south movement of the dominant westerly wind belt in the Southern Hemisphere (Marshall, 2003). Typically, positive SAM phases are associated with winds in the mid-latitudes, while negative SAM phases are associated with winds in the high latitudes. Udy et al. (2021) analyzed synoptic patterns in the southern Indian Ocean around Tasmania and their relationships with modes of climate variability and found relationships between SAM, ENSO, and IOD with certain synoptic nodes, but the SAM exhibited the strongest influence in this region. If the SAM has such a strong impact on weather systems in the southern Indian Ocean, then it likely influences the path of moisture delivery to Mount Read, Tasmania. Positive SAM phases would likely result in a mid-latitude moisture source (associated with more enriched $\delta^{18}O_P$), while negative SAM phases would deliver moisture from higher latitudes (more depleted $\delta^{18}O_P$). Therefore, the difference in source region between years with high $\delta^{18}O_{TR}$ and low $\delta^{18}O_{TR}$ could be influenced by SAM dynamics.

5.4. *Disentangling influences*

Despite the inter-tree variability and some local climate influences,

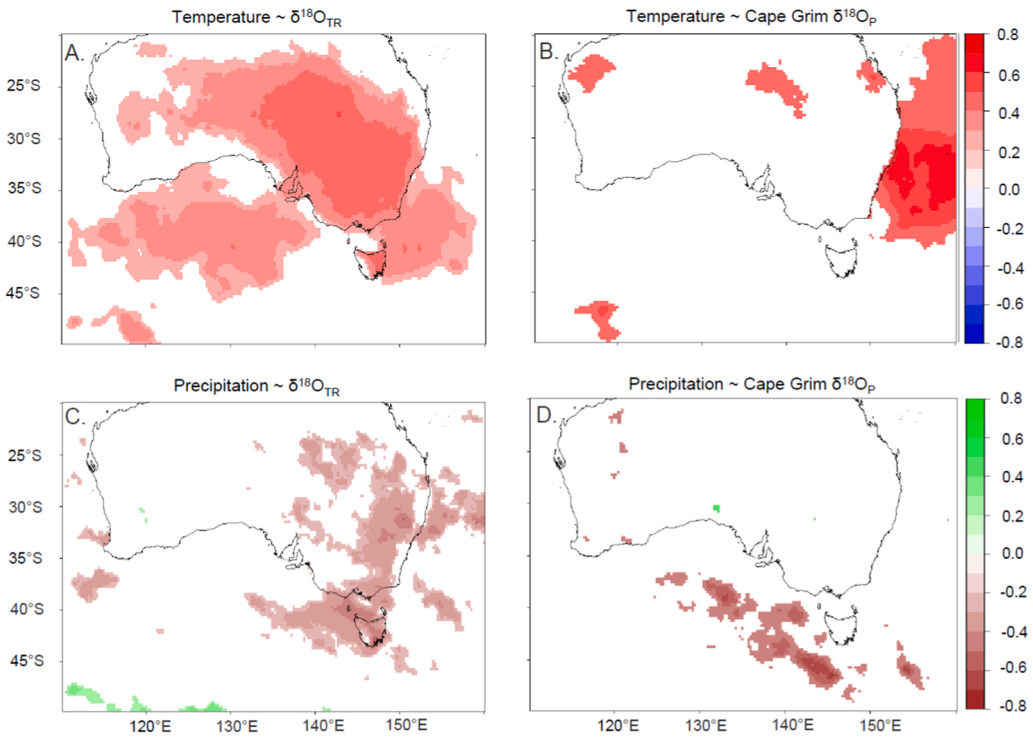

Fig. 6. Spatial maps of Pearson correlations were performed between $\delta^{18}O_{TR}$ and September - February averages of ERA5 temperature at 2 m elevation (A) and total precipitation (C). Also, spatial maps of Pearson correlations were performed between Cape Grim $\delta^{18}O_P$ and September - February averages of ERA5 temperature at 2 m elevation (B) and total precipitation (D). Only statistically significant correlations are displayed ($p < 0.05$).

our results suggest that source region is influential in determining the $\delta^{18}O_{TR}$ signal at Mount Read. While our $\delta^{18}O_{TR}$ record is too variable to reconstruct climate on its own, it shows sensitivity to regional precipitation and temperature, and is broadly similar to measurements of $\delta^{18}O_P$ observed regionally. Therefore, it is possible that these data could be used to represent historical $\delta^{18}O_P$ in Tasmania. A record of historical $\delta^{18}O_P$ may be used in broader reconstructions of climate dynamics such as the SAM and may hint at historical climate conditions dependent upon the relationship between climate variables and $\delta^{18}O_P$.

Given the variation present in the data, we recommend additional data collection to improve the quality of the dataset. The source of variability between trees is most likely local topographic conditions and their influence on rooting depth or a physiological trait in *A. selaginoides* that allows trees to photosynthesize at various times throughout the growing season. Further studies in this region should focus on determining the precise source of variation between trees at Mount Read.

In addition, it is necessary to determine the nature of the source region of precipitation to Mount Read and Tasmania in general, and whether seasonal changes in the source region influence variability in $\delta^{18}O_{TR}$. Dynamical processes that alter source region may influence both local relationships and regional relationships. Future studies focused on developing $\delta^{18}O_{TR}$ records in moist temperate ecosystems should carefully consider the complex influences of local climate conditions, regional climate conditions, and source region precipitation. This can be accomplished by gathering spatially and temporally detailed $\delta^{18}O_P$ data and observing relationships between $\delta^{18}O_P$ and synoptic-scale weather patterns. This analysis would solidify the nature of the linkages between source region dynamics and $\delta^{18}O_P$, and between $\delta^{18}O_P$ and $\delta^{18}O_{TR}$. This knowledge would open the door for more advanced analysis of the influence that large-scale climate dynamics have on the $\delta^{18}O_{TR}$ record.

6. Conclusions

$\delta^{18}O_{TR}$ in *A. selaginoides* at Mount Read maintain weak correlations with local climate measures and slightly stronger correlations with regional climate variables. The weak local controls on $\delta^{18}O_{TR}$ are likely due to high precipitation at Mount Read, resulting in high moisture levels at the site, which strengthens the relationship between $\delta^{18}O_P$ and $\delta^{18}O_{TR}$. The backward trajectories produced by the HYSPLIT model and our regional spatial analysis of precipitation demonstrate that the most influential source region of precipitation at Mount Read is to the west of Tasmania, due to the mid-latitude westerly winds. However, our regional analysis of temperature also points to a potential influence of occasional easterly, low-latitude effects during the growing season. Given the variability between samples and relatively weak relationships with climate variables, $\delta^{18}O_{TR}$ at Mount Read should not be used as a proxy for paleoclimate on its own. However, the $\delta^{18}O_{TR}$ series shows sensitivity to local temperature and VPD, as well as regional temperature and precipitation, meaning that $\delta^{18}O_{TR}$ in *A. selaginoides* has the potential to support paleoclimate reconstructions when combined with other proxies in the region, specifically tree-ring width records in Tasmania. The source region of precipitation to Mount Read is heavily influenced by climate drivers such as the SAM, ENSO, and IOD. Given the sensitivity of the $\delta^{18}O_{TR}$ series to variations in $\delta^{18}O_P$, it is possible that paleoclimate reconstructions involving $\delta^{18}O_{TR}$ at Mount Read and other high latitude Southern Hemisphere locations could provide insight into large-scale climate dynamics.

Declaration of Competing Interest

The authors declare the following financial interests/personal relationships which may be considered as potential competing interests: Amy Hessl reports financial support was provided by National Science Foundation.

Data Availability

Data will be made available on request.

Acknowledgments

This material is based upon work supported by the National Science Foundation P2C2 # 1804121. Laboratory analysis was only possible with the contributions of Autum Downey, Alexis Mueller, Meagan Walker, Ethan Cade, and Kayla Bailey.

Appendix

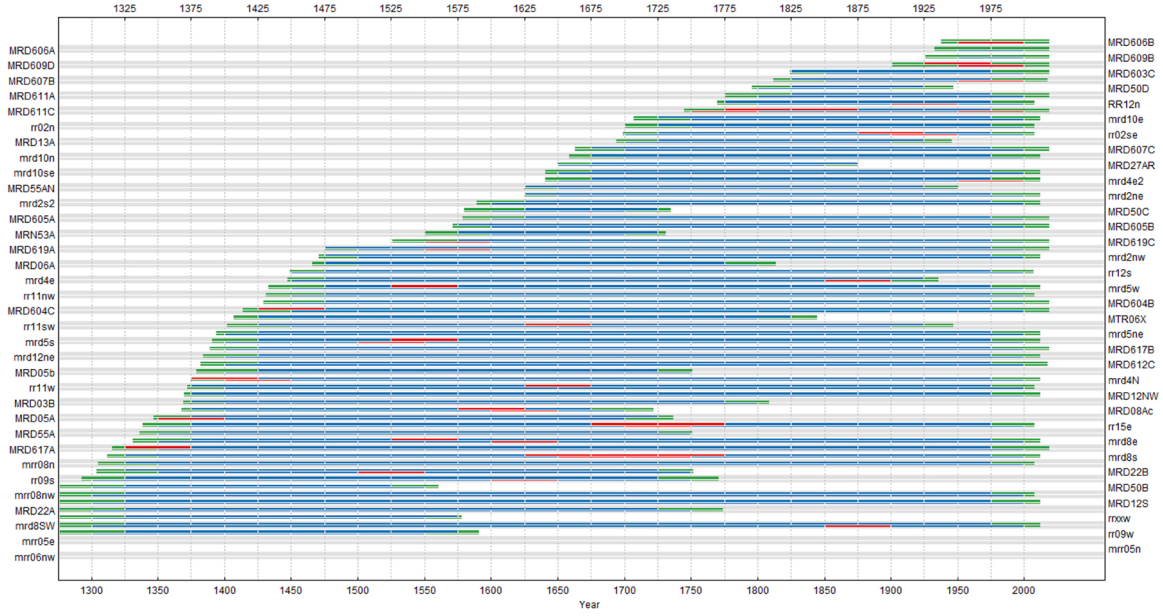

Fig. A1. Correlations between the master chronology (Allen et al., 2017a, 2017b) and each core used in this study for the period of overlap (1308 – 2011). Cores that begin with "MRD6" are cores that were used in isotopic analysis. Correlations are calculated for 50-year segments with a lag of 25 years. Blue segments correlate above the critical value (0.05), red segments correlate below the critical value, green segments are incomplete. The mean correlation with the master chronology for all cores in the Mount Read chronology is 0.533. For the cores used in isotopic analysis, the mean correlation with the master chronology is 0.456.

References

Abram, N.J., Mulvaney, R., Vimeux, F., Phipps, S.J., Turner, J., England, M.H., 2014. Evolution of the Southern Annular Mode during the past millennium. Nat. Clim. Change 4, 564–569. https://doi.org/10.1038/nclimate2235.

Allen, K.J., Nichols, S.C., Evans, R., Allie, S., Carson, G., Ling, F., Cook, E.R., Lee, G., Baker, P.J., 2017. A 277 year cool season dam inflow reconstruction for Tasmania, southeastern Australia. Water Resour. Res. 53, 400–414. https://doi.org/10.1002/2016WR018906.

Allen, K.J., Fenwick, P., Palmer, J.G., Nichols, S.C., Cook, E.R., Buckley, B.M., Baker, P. J., 2017. A 1700-year Athrotaxis selaginoides tree-ring width chronology from southeastern Australia. Dendrochronologia 45, 90–100. https://doi.org/10.1016/j.dendro.2017.07.004.

Barbour, M.M., Roden, J.S., Farquhar, G.D., Ehleringer, J.R., 2004. Expressing leaf water and cellulose oxygen isotope ratios as enrichment above source water reveals evidence of a Péclet effect. Oecologia 138, 426–435. https://doi.org/10.1007/s00442-003-1449-3.

Bell, B., Hersbach, H., Berrisford, P., Dahlgren, P., Horányi, A., Muñoz Sabater, J., Nicolas, J., Radu, R., Schepers, D., Simmons, A., Soci, C., Thépaut, J.-N., 2020. ERA5 monthly averaged data on single levels from 1950 to 1978 (preliminary version).

Boswijk, G., Fowler, A., Lorrey, A., Palmer, J., Ogden, J., 2006. Extension of the New Zealand kauri (Agathis australis) chronology to 1724 BC. Holocene 16, 188–199. https://doi.org/10.1191/0959683606hl919rp.

Brendel, O., Iannetta, P.P.M., Stewart, D., 2000. A rapid and simple method to isolate pure alpha-cellulose. Phytochem. Anal. 11, 7–10. https://doi.org/10.1002/(SICI)1099-1565(200001/02)11:1<7::AID-PCA488>3.0.CO;2-U.

Bureau of Meteorology , 2022. Climate statistics for Australian locations [dataset].

Busby, J.R., & Brown, M.J., 1994. Southern rainforests. Australian vegetation 2, 131–155.

Cook, E., Bird, T., Peterson, M., Barbetti, M., Buckley, B., D'Arrigo, R., Francey, R., Tans, P., 1991. Climatic Change in Tasmania Inferred From a 1089-Year Tree-Ring Chronology of Huon Pine. Science 253, 1266–1268.

Cook, E.R., Peters, K., 1997. Calculating unbiased tree-ring indices for the study of climatic and environmental change. Holocene 7, 361–370. https://doi.org/10.1177/095968369700700314.

Dansgaard, W., 1964. Stable isotopes in precipitation. Tellus 16, 436–468. https://doi.org/10.1111/j.2153-3490.1964.tb00181.x.

Grießinger, J., Langhamer, L., Schneider, C., Saß, B.-L., Steger, D., Skvarca, P., Braun, M. H., Meier, W.J.-H., Srur, A.M., Hochreuther, P., 2018. Imprints of climate signals in a 204 year δ18O tree-ring record of Nothofagus Pumilio from Perito Moreno Glacier, Southern Patagonia (50°S). Front. Earth Sci. 6.

Grzywacz, Z., 2021. Can stable isotopes from tree rings improve our understanding of past variability in the southern annular mode? Grad. Theses Diss. Probl. Rep. https://doi.org/10.33915/etd.10257.

Hendon, H.H., Thompson, D.W.J., Wheeler, M.C., 2007. Australian rainfall and surface temperature variations associated with the southern hemisphere annular mode. J. Clim. 20, 2452–2467. https://doi.org/10.1175/JCLI4134.1.

Hersbach, H., Bell, B., Berrisford, P., Biavati, G., Horányi, A., Muñoz Sabater, J., Nicolas, J., Peubey, C., Radu, R., Rozum, I., Schepers, D., Simmons, A., Soci, C., Dee, D., Thépaut, J.-N., 2019. ERA5 monthly averaged data on single levels from 1979 to present.

Holmes, R.L., 1983. COMPUTER -ASSISTED QUALITY CONTROL IN TREE -RING DATING AND MEASUREMENT 11.

IAEA/WMO , 2021. Global Network of Isotopes in Precipitation [dataset].

Iannone, R., 2016. splitR: Use the HYSPLIT model from inside R.

Jeffrey, S.J., Carter, J.O., Moodie, K.B., Beswick, A.R., 2001. Using spatial interpolation to construct a comprehensive archive of Australian climate data. Environ. Model. Softw. 16, 309–330. https://doi.org/10.1016/S1364-8152(01)00008-1.

Kalnay, E., Kanamitsu, M., Kistler, R., Collins, W., Deaven, D., Gandin, L., Iredell, M., Saha, S., White, G., Woollen, J., Zhu, Y., Chelliah, M., Ebisuzaki, W., Higgins, W., Janowiak, J., Mo, K.C., Ropelewski, C., Wang, J., Leetmaa, A., Reynolds, R., Jenne, R., Joseph, D., 1996. The NCEP/NCAR 40-year reanalysis project. Bull. Am. Meteorol. Soc. 77, 437–472 https://doi.org/10.1175/1520-0477(1996)077<0437:TNYRP>2.0.CO;2.

Lara, A., Villalba, R., 1993. A 3620-year temperature record from fitzroya cupressoides tree rings in Southern South America. Science 260, 1104–1106.

Lavergne, A., Daux, V., Villalba, R., Pierre, M., Stievenard, M., Vimeux, F., Srur, A.M., 2016. Are the oxygen isotopic compositions of Fitzroya cupressoides and Nothofagus pumilio cellulose promising proxies for climate reconstructions in northern Patagonia? J. Geophys. Res. Biogeosciences 121, 767–776. https://doi.org/10.1002/2015JG003260.

Leavitt, S.W., 2010. Tree-ring C–H–O isotope variability and sampling. Sci. Total Environ. 408, 5244–5253. https://doi.org/10.1016/j.scitotenv.2010.07.057.

Marshall, G.J., 2003. Trends in the southern annular mode from observations and reanalyses. J. Clim. 16 (24), 4134–4143. https://doi.org/10.1175/1520-0442(2003)016<4134:TITSAM>2.0.CO;2.

McCarroll, D., Loader, N.J., 2004. Stable isotopes in tree rings. Quat. Sci. Rev. Isot. Quat. Paleoenviron. Reconstr. 23, 771–801. https://doi.org/10.1016/j.quascirev.2003.06.017.

Meier, W.J.-H., Aravena, J.-C., Jaña, R., Braun, M.H., Hochreuther, P., Soto-Rogel, P., Grießinger, J., 2020. A tree-ring δ18O series from southernmost Fuego-Patagonia is recording flavors of the Antarctic Oscillation. Glob. Planet. Change 195, 103302. https://doi.org/10.1016/j.gloplacha.2020.103302.

National Centers for Environmental Prediction/National Weather Service/NOAA/U.S. Department of Commerce , 1994. [dataset] NCEP/NCAR Global Reanalysis Products, 1948-continuing.

Pearman, G.I., Francey, R.J., Fraser, P.J.B., 1976. Climatic implications of stable carbon isotopes in tree rings. Nature 260, 771–773. https://doi.org/10.1038/260771a0.

Porter, T.J., Pisaric, M.F.J., Field, R.D., Kokelj, S.V., Edwards, T.W.D., deMontigny, P., Healy, R., LeGrande, A.N., 2014. Spring-summer temperatures since AD 1780 reconstructed from stable oxygen isotope ratios in white spruce tree-rings from the Mackenzie Delta, northwestern Canada. Clim. Dyn. 42, 771–785. https://doi.org/10.1007/s00382-013-1674-3.

Reid, J.B., 1998. Vegetation of Tasmania. Australian Biological Resources Study.

Roig, F.A., Siegwolf, R., Boninsegna, J.A., 2006. Stable oxygen isotopes (δ18O) in Austrocedrus chilensis tree rings reflect climate variability in northwestern Patagonia, Argentina. Int. J. Biometeorol. 51, 97–105. https://doi.org/10.1007/s00484-006-0049-4.

Stein, A.F., Draxler, R.R., Rolph, G.D., Stunder, B.J.B., Cohen, M.D., Ngan, F., 2015. NOAA's HYSPLIT atmospheric transport and dispersion modeling system. Bull. Am. Meteorol. Soc. 96, 2059–2077. https://doi.org/10.1175/BAMS-D-14-00110.1.

Stokes, M.A., Smiley, T.L., 1968. An Introduction to Tree-ring Dating. University of Arizona Press.

Treble, P.C., Budd, W.F., Hope, P.K., Rustomji, P.K., 2005. Synoptic-scale climate patterns associated with rainfall δ18O in southern Australia. J. Hydrol. 302, 270–282. https://doi.org/10.1016/j.jhydrol.2004.07.003.

Treydte, K., Boda, S., Graf Pannatier, E., Fonti, P., Frank, D., Ullrich, B., Saurer, M., Siegwolf, R., Battipaglia, G., Werner, W., Gessler, A., 2014. Seasonal transfer of oxygen isotopes from precipitation and soil to the tree ring: source water versus needle water enrichment. N. Phytol. 202, 772–783. https://doi.org/10.1111/nph.12741.

Udy, D.G., Vance, T.R., Kiem, A.S., Holbrook, N.J., Curran, M.A.J., 2021. Links between large-scale modes of climate variability and synoptic weather patterns in the Southern Indian Ocean. J. Clim. 34, 883–899. https://doi.org/10.1175/JCLI-D-20-0297.1.

Villalba, R., Lara, A., Masiokas, M.H., Urrutia, R., Luckman, B.H., Marshall, G.J., Mundo, I.A., Christie, D.A., Cook, E.R., Neukom, R., Allen, K., Fenwick, P., Boninsegna, J.A., Srur, A.M., Morales, M.S., Araneo, D., Palmer, J.G., Cuq, E., Aravena, J.C., Holz, A., LeQuesne, C., 2012. Unusual Southern Hemisphere tree growth patterns induced by changes in the Southern Annular Mode. Nat. Geosci. 5, 793–798. https://doi.org/10.1038/ngeo1613.

Zi-Yin, Z., Dao-Yi, G., Xue-Zhao, H., Yang-Na, L., Sheng-Hui, F., 2010. Statistical reconstruction of the Antarctic oscillation index based on multiple proxies. Atmos. Ocean. Sci. Lett. 3, 283–287. https://doi.org/10.1080/16742834.2010.11446883.